

# Learn2Decompose: Learning Problem Decomposition for Efficient Task and Motion Planning

Yan Zhang<sup>1,2</sup> Amirreza Razmjoo<sup>1,2</sup> Sylvain Calinon<sup>1,2</sup>  
<sup>1</sup>Idiap Research Institute <sup>2</sup>EPFL  
 {name.surname}@idiap.ch

**Abstract:** We focus on designing efficient Task and Motion Planning (TAMP) approach for long-horizon manipulation tasks involving multi-step manipulation of multiple objects. TAMP solvers typically require exponentially longer planning time as the planning horizon and the number of environmental objects increase. To address this challenge, we first propose Learn2Decompose, a Learning from Demonstrations (LfD) approach that learns embedding task rules from demonstrations and decomposes the long-horizon problem into several subproblems. These subproblems require planning over shorter horizons with fewer objects and can be solved in parallel. We then design a parallelized hierarchical TAMP framework that concurrently solves the subproblems and concatenates the resulting subplans for the target task, significantly improving the planning efficiency of classical TAMP solvers. The effectiveness of our proposed methods is validated in both simulation and real-world experiments.

**Keywords:** Learning for Task and Motion Planning, Learning Rules from Demonstrations, Learning Problem Decomposition

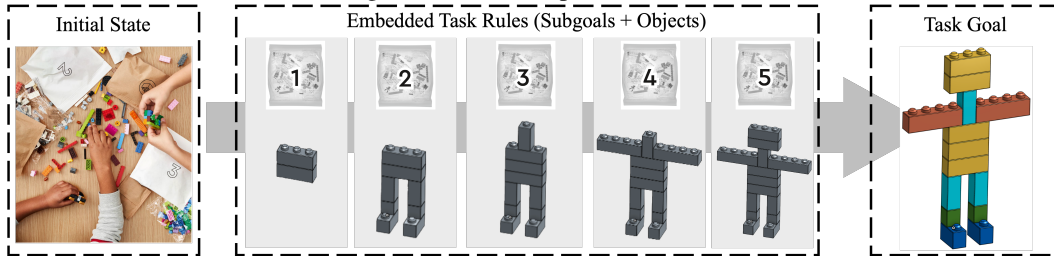


Figure 1: **Motivation of Learn2Decompose.** Long-horizon manipulation tasks typically adhere to embedded task rules. For example, the instruction manual (the middle one of the blocks with dashed outlines) for a simplified robot assembly task indicates key subgoals and the essential blocks required for achieving each subgoal. By leveraging such a manual, the task can be divided into several subproblems (each grey block) that can be accomplished by several individuals concurrently. Subsequently, the plans for those subproblems can be integrated based on their sequence to achieve the overall task goal, regardless of the initial state.

## 1 Introduction

Numerous daily activities, from cooking [1] to furniture assembly [2], demand long-horizon manipulation planning. These tasks often involve complex interactions among robots and many objects under spatial-temporal constraints, and planning over long horizon with sparse rewards [3, 4, 5], presenting significant challenges for autonomous robotic solutions. Recently, Task and Motion Planning (TAMP) has emerged as a powerful framework for tackling these complex long-horizon manipulation tasks [1, 3]. TAMP integrates task planning with motion planning by combinatorially searching sequences of abstracted actions and corresponding motion trajectories [6, 7, 8]. Consequently, as the planning horizon and the number of environmental objects grow, TAMP solvers require exponentially longer planning time [1, 9, 10]. It is still an open issue to design efficient TAMP frameworks for solving long-horizon manipulation tasks.

A considerable amount of long-horizon manipulation tasks usually adhere to embedding task rules that facilitate their completion. For instance, cooking a meal can consistently follow a recipe, regardless of the initial placement of the ingredients; similarly, assembling furniture can adhere to an instruction manual, irrespective of how the components are packaged. Moreover, by leveraging these rules, it is possible to decompose the long-horizon manipulation tasks into several simpler subproblems, which can first be tackled in parallel by multiple individuals and then concatenated to address the overarching task, as shown in Figure 1. This paper proposes an efficient parallelizable hierarchical TAMP approach based on this concept by answering the following three questions:

- How can the embedded task rules of a long-horizon manipulation task be generated?
- How can the task be decomposed into several subproblems that can be solved in parallel?
- How can we design an efficient TAMP approach with the decomposed subproblems?

Learn2Decompose answers the first question by defining the embedding task rules of a multi-step manipulation task in terms of sequential subgoals and key objects necessary to achieve each subgoal. The subgoals are identified through a novel learning from symbolic demonstrations method which extract bottleneck symbolic states in an unsupervised manner. The important objects are identified using an existing GNN-based (Graph Neural Network) object importance prediction function [9]. More importantly, we show that combining with the learned subgoals, this importance prediction function can be utilized for the decomposition of the task into several subproblems that can be solved in parallel. This capability then facilitates the design of an efficient parallelized hierarchical TAMP framework for long-horizon manipulation tasks with different initial conditions, answering the third question.

In summary, the main contributions of this paper are as follows:

- Introducing a parallelized hierarchical TAMP approach that efficiently addresses long-horizon manipulation tasks under various initial conditions.
- Proposing Learning2Decompose, a problem decomposition method that decomposes long-horizon planning problems into several subproblems, which can be solved in parallel.
- Developing a new learning from demonstrations method that extracts symbolic subgoal-defined rules from a few demonstrations in an unsupervised manner.

## 2 Related Work

**Learning Rules from Demonstrations:** Classical Learning from Demonstrations (LfD) has demonstrated that task rules can be extracted from symbolic demonstrations [11, 12, 13]. With predefined actions/controllers, these methods extract sequential key actions as symbolic rules for imitating humans’ behaviors. However, the resulting action rules vary with different action abstractions, even if the state abstraction remains consistent. LfD algorithms [14, 15, 16] can also learn rules defined by temporal logic with proper proposition abstraction, though this often requires deep expertise about the target tasks. Unlike these approaches, our method generates subgoal-defined symbolic rules from demonstrations using only state abstraction, which can be obtained with existing scene graph generating techniques [17, 18], thus eliminating the dependency on action/proposition abstraction.

**Exploring Subgoals for Long-horizon Manipulation Planning:** In Reinforcement Learning (RL), subgoals are often identified by segmenting motion-level trajectories and used as a reward densifying technique for long-horizon manipulation planning with sparse reward [4, 5, 19, 20, 21, 22, 23]. Unlike these methods, our approach aims to improve the computation time of TAMP solvers using symbolic demonstrations to identify subgoals. Recently, Levit et al. [24] suggested identifying subgoals in the bottleneck region of the environment to improve the resolution of 2D puzzle problems with optimization-based TAMP solvers. In their work, the subgoals primarily aim to alleviate local optima issues in optimization-based motion planning. Differently, we aim to extract subgoals from a few symbolic demonstrations to shorten the planning horizon and enhance planning efficiency.

**Learning for Efficient TAMP:** TAMP solvers typically face exponentially longer planning time as the planning horizon and the number of manipulable objects grow [10, 1]. To mitigate this, imitation learning methods have been employed to learn long-horizon planning policies from large-scale demonstrations generated with TAMP solvers [25, 26]. Although these methods demonstrate impressive online inference efficiency, they depend heavily on the offline collection of a vast number of diverse demonstrations, and their performance tends to decline with increasing task complexity. In contrast, robot learning methods can be used to learn heuristics from a small number of demonstrations to speed up long-horizon planning. These methods include learning value functions as cost-to-go heuristics [27] and learning action feasibility [28, 29, 1] to prune infeasible branches without expensive motion planning validation, thus speeding up TAMP solvers. Moreover, the importance of objects or their associated streams is predicted to streamline the planning process [9, 30]. Our approach integrates the object importance prediction function in [9] to filter out non-essential objects, and more importantly to effectively decompose a long-horizon manipulation problem into several parallelly solvable subproblems.

**Exploring Parallelizable Decomposition for Efficient TAMP:** Leahy et al. [31] propose to decompose multi-agent path planning problems with global temporal logic goals into smaller subproblems, employing a set of heuristic rules arising from temporal logic specifications. Hartmann et al. [3] manually decompose long-horizon construction planning into subproblems where one object and multiple robots are involved in and solve them sequentially. These works share the same motivation to ours, but their decomposition methods primarily depend on the heuristics arisen from task [3] or goal specifications [31]. Instead, in this work, we aim to provide a generic framework that automates problem decomposition.

**Exploring Hierarchy for Efficient TAMP:** The use of hierarchical structures has been beneficial for enhancing long-horizon manipulation planning, primarily through expert-designed higher-level action abstraction. For example, Elimelech et al. [32] propose to generate higher-level action abstraction upon those from PDDL by solving an optimization-based key states detection methods to speed up task planning [32, 33]. Kaelbling and Lozano-Perez [10], Driess et al. [34] propose hierarchical TAMP frameworks by manually defining the action abstraction with different hierarchies. Our method is a novel hierarchical TAMP framework that constructs hierarchy in a top-down fashion through problem decomposition, as opposed to the traditional bottom-up approach via action abstraction. Moreover, compared to [10, 34], our method finds the hierarchy automatically from demonstrations, alleviating the difficulty in manually defining action abstractions with hierarchies.

### 3 Learn2Decompose for Efficient Parallelized Hierarchical TAMP

In this section, we present Learn2Decompose and the parallelized hierarchical TAMP approach for efficient long-horizon manipulation planning. An overview of our proposed methods is illustrated in Figure 2. Learn2Decompose involves both offline and online stages in Figure 2. In offline phase, it generates a sequence of subgoals from demonstrations and trains a GNN model to predict the importance of objects during transitions between consecutive subgoals; In online phase, it generates parallelly solvable subproblems based on the predicted importance of objects. The parallelized hierarchical TAMP refers to the online planning process where TAMP solvers are run concurrently to generate subplans for each subproblem. These subplans are then concatenated to efficiently solve the overall task. In the following, we detail each of these components in order.

#### 3.1 Background

**Planning Domain Definition Language (PDDL)** provides abstractions for both state and action in task planning scenarios. For example, consider subgoal  $G'_2$  depicted in Figure 2: cube E is atop of cube F denoted as (*on E F*), and there are no other cubes above cube E, expressed as (*clear E*). In this paper, we use the term *scene graph* to collectively represent the entire set of states. An action in PDDL is defined by its preconditions, effects, and parameters. Preconditions must be satisfied before the action can be executed, while parameters specify the entities involved in the action (*e.g.* robots

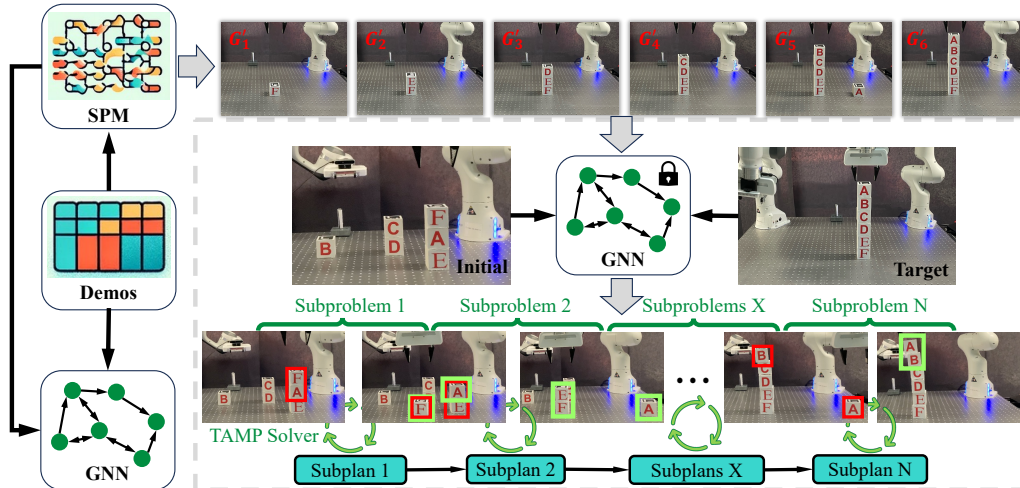


Figure 2: **Overview of Learn2Decompose and the parallelized hierarchical TAMP approach.**

Learn2Decompose, depicted outside the grey block, involves an offline process that extracts the subgoals  $G'_i$  from demonstrations by formulating the problem as a Sequential Pattern Mining (SPM) problem. It also trains a Graph Neural Network (GNN) offline to generate online **subproblems** that are parallelly solvable. The grey block represents the online phase, where the task is decomposed into several subproblems that are concurrently solved with **TAMP solvers**. Each subproblem is illustrated by two consecutive images: the first image uses red blocks to highlight important objects, and the second image uses green blocks to represent the goal configurations. All non-essential objects are virtually merged with the table to facilitate correct motion planning. The resulting subplans are then concatenated according to the subproblem order to tackle long-horizon manipulation tasks with a consist target, but varying initial states.

and objects), and effects denote the resulting states after the action is executed. For example, an instance of the action *pick* may involving pick up cube F from the table, with preconditions (*clear F*) and (*empty arm*), parameters (*arm, F*), and effects (*inhand F*). While PDDL planners excel at task planning, they do not consider the corresponding motion trajectories required to achieve the planned subtasks.

**PDDLStream** [8] extends PDDL by incorporating streams, which sample continuous parameters subject to constraints and output static facts *certifying* that these parameters satisfy the constraints [35]. This enables PDDLStream to simultaneously solve task and motion planning problems. For example, to *pick* cube E, PDDLStream can define streams such as *grasp-pose* and *collision-free-trajectory*. The former samples feasible grasping poses for cube E, while the latter generates collision-free robot trajectories for reaching those poses. The resulting static facts (*hand-pose ?g*) and (*cfree ?t*) augment the preconditions for the action *pick*. Given the domain and stream definitions, along with initial facts, PDDLStream utilizes a PDDL planner to determine if the task goal can be achieved with the current set of facts. If not, it iteratively generates additional facts using streams and verifies the attainment of the task goal with the expanded set of facts, until feasible task and motion plans are found to accomplish the task goal.

**Dynamic Movement Primitives (DMP)**, as a classical LfD method, can generalize one demonstrated trajectory to different initial and goal poses, demonstrating promising extrapolation generalization capability [36, 37]. Besides, the optimal control formulation of DMP, as shown in [38, 39], offers expressive via-point modulation capability, which is beneficial for collision avoidance and contact-rich manipulation subtasks. In this letter, we leverage both the extrapolation generalization and via-point modulation capabilities of DMP to generate smooth, collision-free motion trajectories for connecting feasible grasping pose provided by PDDLStream. For a given set of abstracted actions, we utilize the collected geometric demonstrations  $\{\mathcal{P}_i^g\}_{i=1,\dots,N}$  to train DMPs for each action.

### 3.2 Preliminary

**Problem Formulation.** Our objective is to learn generic task rules that accelerate TAMP solvers within the same state abstraction, but possibly different action abstraction. To achieve this, we define the task rules as a sequence of key states (subgoals) and key objects that are involved during transitions between two consecutive key states, as shown in Figure 1. We aim to generate these key states and objects from a limited number of task demonstrations and integrate these task rules into TAMP solvers for efficient long-horizon planning.

**Assumptions.** We assume access to sensors capable of capturing the poses of robots and environmental objects, and a set of rules that translate these geometrical states into predefined PDDL predicates representing their symbolic states. With the learned generic task rules, we then apply a specific action abstraction to run a designated TAMP solver for the target tasks. We also assume a set of known stream functions for using PDDLStream as our TAMP solver. Moreover, we assume that different tasks share the same task goal  $G$  but vary in their initial states.

**Demonstrations Collection.** Using the defined rules and abstracted symbolic states, we generate a small set of demonstrations that successfully achieve the task goal  $G$  across  $N$  distinct initial states. Here we employed PDDLStream to generate 100 sequences of geometrical states  $\{\mathcal{P}_i^g\}_{i=1,\dots,N}$  of robots and objects by varying the initial environment configuration. However, it is important to note that these demonstrations can also be derived from human demonstration or videos. Based on the rules and abstracted states, we then produced the corresponding symbolic demonstrations  $\{\mathcal{P}_i^s\}_{i=1,\dots,N}$ . These demonstrations, denoted as  $\mathcal{P}$ , include both symbolic and geometrical state trajectories  $\{\mathcal{P}_i^s, \mathcal{P}_i^g\}_{i=1,\dots,N}$ .

**Graph Representation of Demonstrations.** We represent the environment configurations as scene graphs based on the state abstraction with PDDL, as illustrated in Figure 3. In each scene graph, objects are modeled as nodes, with their internal logical states as node features. These internal states encompass both symbolic and geometrical states like whether an object is *clear* and its positions. The external logical states of an object, which indicate relationships with other objects, *e.g.* *on* are modeled as edge features.

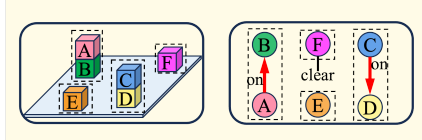


Figure 3: Illustration of a scene graph represented as subgraph sets. In the right figure, each dashed outline encloses the corresponding subgraphs. Only representative symbolic state descriptions (*e.g.*, *on*, *clear*) are shown.

### 3.3 Learn2Decompose

In this section, we present Learn2Decompose by addressing three essential questions: 1) How to learn subgoals from demonstrations; 2) How to train the GNN model to predict the importance of objects; 3) How to generate parallelly solvable subproblems based on the predicted importance of objects.

**Learning subgoals from demonstrations.** To extract subgoals from demonstrations, we first transform each scene graph  $\mathcal{G}_j$  into a set of subgraphs  $\{\mathcal{H}_k\}_{k=1,\dots,k_j}$ , based on the connectivity of its nodes as illustrated in the right of Figure 3. Here,  $k_j$  represents the number of subgraphs derived from the  $j$ -th scene graph in the demonstration  $\mathcal{P}_i$ . Consequently, each demonstration  $\mathcal{P}_i = \{\mathcal{P}_i^s, \mathcal{P}_i^g\}$  can be represented as a sequence of subgraph sets  $\{\{\mathcal{H}_k\}_{k=1,\dots,k_j}\}_{j=1,\dots,l_i}$  where  $l_i$  denotes the length of  $\mathcal{P}_i$ . Given the demonstrations represented as  $N$  sequences of subgraph sets, we first identify sequences of subgraph sets that are common across all demonstrations. Then, from these common sequences, we select the one that encompasses maximal information to define the target sequential subgoals.

The common subgraph sets sequences are derived by framing the problem as a sequential pattern mining (SPM) problem [40], where each scene graph is treated as an element and its corresponding subgraphs as items within that element. To solve this SPM problem, we employ PrefixSpan [41, 42], an off-the-shelf SPM algorithm renowned for its simplicity and flexibility in incorporat-

ing constraints (*e.g.*, max) [40]. Specifically, given the symbolic demonstrations  $\{\mathcal{P}_i^s\}_{i=1,\dots,N}$  as a database consisting of  $N$  sequences of subgraph sets, PrefixSpan identifies all sequences of subgraph sets  $\mathcal{H} = \{\{\mathcal{H}_k\}_{k=1,\dots,k_m}\}_{m=1,\dots,M}$  that meet or exceed a minimum occurrence frequency ratio, defined as *min-support*. Here,  $k_m$  represents the number of common subgraph sets extracted from similar scene graphs.  $M$  indicates the total number of interesting sequential patterns. We set *min-support* = 0.9, targeting those sequential subgraph sets that appear in at least 90% of the demonstrations for each experiment (see [41] for more details on PrefixSpan).

Using PrefixSpan, we generate a set of subgraph sequences including both the target subgoal sequence  $\mathbf{G}' = \{\mathbf{G}'_1, \dots, \mathbf{G}'_Z\}$  and its subsequences, where  $Z$  is an unknown variable representing the length of the target sequence and lies within the range  $[1, l_i^{\min}]$  ( $l_i^{\min}$  is the shortest length of demonstrations). We then distinguish the target sequence of subgoals  $\mathbf{G}'$  from its subsequences by choosing the one with maximal information. The information metric is defined as the composition of three terms: the sequence length  $R_l$ , the total number of subgraphs  $R_q$ , and the count of distinct subgraphs  $R_v$ . The components  $R_q$  and  $R_v$  are specifically designed to distinguish the target sequence from other sequences of the same length that consist of only subsets of the common subgraphs, denoted by  $\hat{\mathbf{G}}' = \{\hat{\mathbf{G}}'_1, \dots, \hat{\mathbf{G}}'_Z\}$ , where  $\hat{\cdot}$  indicates a subset of the corresponding item. We then maximize the reward function:  $R = R_l + R_q + R_v$  to identify and generate the target sequence of subgoals  $\mathbf{G}'$ .

**Training the GNN-based importance prediction function.** Given the sequence of subgoals  $\mathbf{G}'$ , we divide each demonstration into segments that include both the symbolic and geometrical state trajectories, transiting from one subgoal  $\mathbf{G}'_i$  to the next  $\mathbf{G}'_{i+1}$ . With these segments, we identify important objects for each subgoal transition process by analyzing the changes in object states. Objects whose states change during the transition are considered important. We use the entire scene graphs while the environment is at subgoal  $\mathbf{G}'_i$  and  $\mathbf{G}'_{i+1}$  as inputs, and the identified important objects as outputs, to construct a graph dataset for training the GNN model. This GNN model is then utilized online to predict important objects during transition from  $\mathbf{G}'_i$  to  $\mathbf{G}'_{i+1}$ . The training follows the pipeline outlined in [9] with key differences: our model incorporate geometric states of objects, such as their positions, as part of the node features; Additionally, unlike [9], which aims to predict important objects for the entire task, our approach assumes such set of objects is known as prior and focuses on predicting important objects specifically between two subgoals.

**Parallely solvable subproblem generation.** In this section, we describe the process for generating parallely solvable subproblem based on the sequence of subgoals and the trained GNN model. To solve each subproblem concurrently, it is necessary to know the initial and goal states of each subproblem in advance. However, the initial states  $L_1$  for subproblem  $SP'_2$  (aiming to reach subgoal  $\mathbf{G}'_2$ ) are derived from the end states of subproblem  $SP'_1$  for subgoal  $\mathbf{G}'_1$ , starting from state  $L_0$ . For the same subgoal  $\mathbf{G}'_1$ , the environment may transit to different end states  $L_1$  or  $L'_1$  or  $L''_1$  depending on the starting state  $L_0$  or  $L'_0$  and the planned action skeleton, as shown in Figure 4. To address this issue, we propose to leverage the predicted importance of objects from the trained GNN model to generate parallely solvable subproblems.

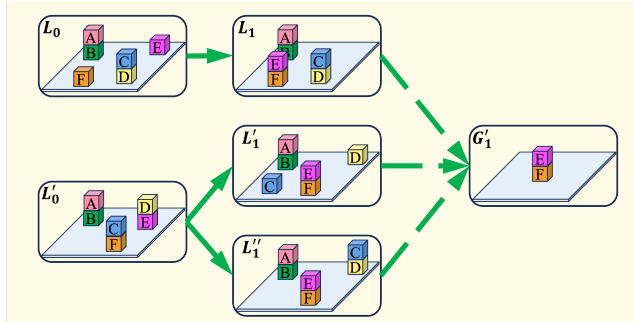


Figure 4: From two different initial states  $L_0$  and  $L'_0$ , TAMP may reach different states  $L_1$  and  $L'_1$  for achieving the subgoal  $\mathbf{G}'_1$ . Moreover, with the same initial state  $L'_0$  and subgoal  $\mathbf{G}'_1$ , TAMP solvers may reach different states  $L'_1, L''_1$ . Therefore, reaching subgoals are not parallelizable.

For a new task starting from initial state  $L'_0$  and aiming for the task goal  $\mathbf{G}$ , we initiate the subproblem generation process by predicting important objects (*e.g.*, cubes  $C, D, E, F$ ) from  $L'_0$  to the first

subgoal  $G'_1$ , as shown in Figure 4. Since the expected configurations for some important objects (e.g.,  $E, F$ ) are already specified in subgoal  $G'_1$ , we can precisely determine the states of cubes  $E, F$  if subproblem  $SP'_1$  is successfully completed. For other important objects (e.g.,  $C, D$ ) not in subgoal description, additional configurations must be specified to ensure that the entire environment reaches a deterministic configuration at the end of  $SP'_1$ . This can be achieved by isolating cubes  $C$  and  $D$  as separate subgraphs and assigning random feasible poses to them based on their resulted symbolic states, resulting in  $L'_1$  in Figure 4. Consequently, the goal for subproblem  $SP'_1$  becomes achieving subgoal  $G'_1$  and placing cubes  $C$  and  $D$  on table at assigned poses.

Although cubes  $A, B$  are not crucial for achieving the subproblem goal, their geometric properties, such as shape, influence the feasibility of motion-level states. For instance, the shapes of cubes  $A, B$  influence the feasible areas for sampling collision-free placement positions for cubes  $C, D$  on the table. To address this, we propose merging the geometric information of non-important objects with the base environment (the table) as a virtual base. This approach ensures that object reduction does not impact motion planning in subproblem  $SP'_1$ . Therefore, goal description for subproblem  $SP'_1$  is updated to  $L'_1$  with cubes  $A, B$  virtually merged with the blue table.

With subproblem  $SP'_1$ , we then determine the initial states  $L'_1$  for the next subproblem  $SP'_2$  by combining the goal description of  $SP'_1$  and the states of non-important objects for subproblem  $SP'_1$  that remain unchanged for  $L'_0$  to  $L'_1$ . This process iteratively continues until all subproblems are well-defined for reaching the task goal  $G$ .

### 3.4 Efficient Parallelized Hierarchical TAMP

In this section, we present the parallelized hierarchical TAMP approach, specifically designed to efficiently address long-horizon manipulation tasks characterized by a consistent task goal  $G$  and varying initial states  $L_0$ .

As summarised in Algorithm 1. The environment  $env$ , the demonstrations  $\mathcal{P}$  and task goal  $G$  are presumed to be known. In this work, we select PDDLStream [8] as the TAMP solver to generate feasible key robot poses and utilize trained DMPs for each abstracted actions to produce smooth, collision-free trajectories. Note that both DMP and PDDLStream can be replaced with other methods that provide equivalent functionalities. The intended output includes an action skeleton  $\mathbf{a} = \{a_u\}_{u=1,\dots,U}$ , coupled with corresponding motion trajectories  $\boldsymbol{\tau} = \{\tau_u\}_{u=1,\dots,U}$  where  $U$  denotes the length of the planned action sequence.

Moreover, in anticipation of the actual task planning, the subgoals  $G'$  and a GNN-based scoring function  $\mathcal{V}$  are precomputed with methods outlined in Section 3.3.

When online addressing a new task starting from  $L_0$ , the function *SubproblemsGen* decomposes the task into several subproblems  $SP = \{SP_z\}_{z=1,\dots,Z}$ , where  $Z$  indicates the number of subgoals and subproblems. Objects that attain an importance score exceeding the score threshold  $\gamma \in (0, 1)$  are identified as crucial objects for the corresponding subproblem. If the TAMP solver fails to find a solution for any of the subproblems, we terminate the *ParallelTAMP* process and switch to *SequentialTAMP* where we aim to reach each subgoals without object reduction and parallelization. One can also explore the incremental planning strategy presented in [9] to reduce the threshold  $\gamma$ , such as setting  $\gamma \leftarrow \gamma^2$ . Successful resolution of all subproblems leads to the concatenation of SubPlans to address the target task, adhering to the sequence of subgoals.

---

#### Algorithm 1: Parallelized Hierarchical TAMP

---

**Given :** Environment  $env$ , Demonstrations  $\mathcal{P}$ , Task Goal  $G$ , Skills  $\mathcal{A}$ , Score Thresholds  $\gamma$

**Output:** Action Skeleton  $\mathbf{a}$  and Motions  $\boldsymbol{\tau}$

**Offline:**

$G' \leftarrow \text{SubgoalsGen}(\mathcal{P}, G)$   
     $\mathcal{V} \leftarrow \text{GNN}(\mathcal{P}, G')$

**Online:**

$L_0 \leftarrow \text{SceneGraph}(env)$   
     $SP \leftarrow \text{SubproblemsGen}(L_0, \mathcal{V}, \gamma, G')$   
    SubPlans  $\leftarrow \text{ParallelTAMP}(SP)$   
    **if None in SubPlans then**  
        SubPlans  $\leftarrow \text{SequentialTAMP}(G')$   
     $\mathbf{a}, \boldsymbol{\tau} \leftarrow \text{Concatenate}(\text{SubPlans}, \mathcal{A})$

---

**Subplan Concatenation.** With PDDLStream, we first generate the key robot poses required for object manipulation. Subsequently, we create corresponding smooth, collision-free motion trajectories  $\tau_v$  by exploring the generalization and via-point modulation capabilities of DMP trained for each abstracted action. This approach facilitates the concatenation of subplans at motion level.

In summary, the proposed Learn2Decompose approach decomposes a long-horizon manipulation task into parallelizable, shorter-horizon subproblems with less environmental objects involved. The further developed parallelized hierarchical TAMP method efficiently addresses the long-horizon problem by integrating Learn2Decompose, which facilitates the exploration of subgoals, object reduction, and parallelization. In the following Experiments section, we demonstrate how these three features enhance the planning efficiency of TAMP solvers.

## 4 Experiments

### 4.1 Environment Setups

We validated the proposed methods using two common TAMP benchmarks: block stacking and cooking in the kitchen. For each scenario, we tested the performances of our methods in different tasks which involved in different number of objects, thus different planning horizons. In the following, we illustrate the performance of Learn2Decompose in terms of subgoal generation and object reduction, and compare the efficiency of the parallelized hierarchical TAMP with several baselines. Please refer to Appendix A.3 for more detailed task descriptions.

### 4.2 Simulation Experiment Results

In this section, we select PDDLStream [8] as the TAMP solver and compare parallelized hierarchical PDDLStream (**PS+PL**) with PDDLStream (**PS**), PDDLStream with subgoals generated from SPM (**PS+SPM**), PDDLStream with sequential subproblems (**PS+SPM+GNN**) solving. The comparison are made in terms of planning horizon, number of objects involved in each subproblem, and the resulting planning efficiency, as shown in Tables 1, 2, 3. In this context, **PS+SPM** refers to the *SequentialTAMP* function in Algorithm 1 where each subgoal is reached sequentially; **PS+SPM+GNN** refers to sequentially solving each parallelizable subproblem, where both subgoals and GNN-based object reduction are used. This comparison is designed to highlight the acceleration achieved through object reduction and the impact of parallelization, which is fully explored in our proposed method. For clarity, we refer to **PS+PL** as **ours** in the following tables. For each method and task goal, we run 100 trials with different random seed than the one used for training the corresponding GNN model. In each trial, the environment configurations were randomly initialized. The average values and standard deviations are reported in the following tables.

	<b>PS</b>	<b>PS+SPM</b>	<b>PS+SPM+GNN</b>	<b>ours</b>
<b>Block4</b>	8.30 ± 2.66	<b>2.44 ± 0.48</b>	2.75 ± 1.40	2.75 ± 1.40
<b>Block6</b>	15.44 ± 3.98	<b>2.70 ± 0.54</b>	3.20 ± 2.43	3.20 ± 2.43
<b>Block8</b>	23.02 ± 4.61	<b>2.78 ± 0.43</b>	3.30 ± 2.90	3.30 ± 2.90
<b>Cook3</b>	10.57 ± 1.47	<b>1.76 ± 0.25</b>	1.77 ± 1.0	1.77 ± 1.0
<b>Cook4</b>	13.95 ± 1.70	<b>1.74 ± 0.21</b>	1.75 ± 0.19	1.75 ± 0.19
<b>Cook5</b>	17.52 ± 1.87	<b>1.75 ± 0.19</b>	1.75 ± 0.97	1.75 ± 0.97

Table 1: Comparison of planning horizon. **PS+SPM+GNN** and **ours** refer to the same subproblems, and thus they share the same planing horizon.

**Learn2Decompose facilitates problem decomposition.** Problem decomposition includes both goal decomposition and object reduction. In Tables 1 and 2, we present a comparison of the average planning horizon and number of objects across different methods and tasks. Notably, Learn2Decompose effectively breaks down complex manipulation tasks with planning horizon ranging from 8 to 24 and involving 6 to 13 objects into subproblems requiring a mere 2 to 4 planning horizons and involvement of only 2 to 5 objects. Furthermore, the average planning horizon and the number of objects involved in each subproblem only increase slightly with growing problem com-



	<b>PS</b>	<b>PS+SPM</b>	<b>PS+SPM+GNN</b>	<b>ours</b>
<b>Block4</b>	6 ± 0	6 ± 0	<b>2.13 ± 0.60</b>	<b>2.13 ± 0.60</b>
<b>Block6</b>	8 ± 0	8 ± 0	<b>2.43 ± 0.98</b>	<b>2.43 ± 0.98</b>
<b>Block8</b>	10 ± 0	10 ± 0	<b>2.58 ± 1.36</b>	<b>2.58 ± 1.36</b>
<b>Cook3</b>	9 ± 0	9 ± 0	<b>3.92 ± 0.77</b>	<b>3.92 ± 0.77</b>
<b>Cook4</b>	11 ± 0	11 ± 0	<b>3.98 ± 0.74</b>	<b>3.98 ± 0.74</b>
<b>Cook5</b>	13 ± 0	13 ± 0	<b>4.23 ± 1.21</b>	<b>4.23 ± 1.21</b>

Table 2: Comparison of number of objects. **PS+SPM+GNN** and **ours** refer to the same subproblems, and therefore share the same number of objects. Besides, the number of objects for **PS** and **PS+SPM** remains fixed, since no object reduction is involved in both methods.

	<b>PS</b>	<b>PS+SPM</b>	<b>PS+SPM+GNN</b>	<b>ours</b>
<b>Block4</b>	1.87 ± 0.59	2.39 ± 0.59	1.53 ± 0.13	<b>0.51 ± 0.11</b>
<b>Block6</b>	9.65 ± 4.44	5.56 ± 0.87	2.35 ± 0.24	<b>0.75 ± 0.23</b>
<b>Block8</b>	191.80 ± 19.75	11.39 ± 1.11	4.16 ± 1.58	<b>1.65 ± 1.30</b>
<b>Cook3</b>	0.82 ± 0.06	2.08 ± 0.08	0.73 ± 0.03	<b>0.18 ± 0.02</b>
<b>Cook4</b>	1.42 ± 0.09	4.52 ± 0.11	1.61 ± 0.10	<b>0.31 ± 0.05</b>
<b>Cook5</b>	2.26 ± 0.16	8.86 ± 0.21	2.43 ± 0.27	<b>0.45 ± 0.15</b>

Table 3: Comparison of planning time cost [s]

plexity. As a result, the planning time of our proposed methods shows only a modest increase as task complexity rises, as shown in Table 3. This outcome underscores the motivation behind proposing Learn2Decompose and demonstrates its effectiveness in problem decomposition.

**Parallelized hierarchical TAMP significantly improves planning efficiency.** Table 3 outlines the comparative planning efficiency among different methods. Our proposed parallelized hierarchical TAMP greatly boosts planning efficiency by over 78% for the **Cook-X** tasks and achieves smaller computation time by two orders of magnitude for the most complex **Block-X** task. While **PS+SPM+GNN** and **PS+SPM** also show improvements in planning efficiency for the **Block-X** tasks, they do not consistently guarantee speed improvement. Notably, **PS+SPM** exhibits longer planning times than using PDDLStream alone in the **Block4** task and all the **Cook-X** tasks. This discrepancy arises from the planning principle of PDDLStream, which iteratively conducts stream sampling and action skeleton search with previously sampled streams. In contrast, **PS+SPM** and **PS+SPM+GNN** treat each subgoal-reaching problem or subproblem as a new TAMP problem, requiring a solution from scratch without leveraging previously sampled streams. Our method alleviates this issue through parallelization, consistently enhances planning efficiency. This underscores our motivation for designing a parallelized hierarchical TAMP approach that not only focuses on subgoal generation and object reduction but also on generating concurrently solvable subproblems for parallelization.

### 4.3 Real-world Experiments

We validated the effectiveness of our methods for **Block6** tasks under various initial states in real-world settings. All experiments were conducted using a 7-axis Franka robot arm, equipped with a RealSense D435 camera for object localization. The Learn2Decompose approach successfully decomposed the tasks into several subproblems and our parallelized hierarchical TAMP method concurrently found subplans for each subproblems, which were then concatenated to achieve the target tasks. Please refer to Appendix A.4 for more detailed description of real-world experiment results.

## 5 Conclusion and Limitations

In summary, we proposed Learn2Decompose, an LfD algorithm that discovers task rules from a few demonstrations. These task rules include a sequence of subgoals and key objects during transitions between two consecutive subgoals, and facilitate to decompose a long-horizon manipulation task

into several subproblems. These subproblems require shorter planning horizons, involve fewer objects, and more importantly can be solved in parallel. This thus enables us to construct an efficient, parallelized hierarchical TAMP approach which significantly improves the planning efficiency of TAMP solvers. We validated the proposed methods through simulations and real-world applications, confirming their effectiveness in decomposing problems and improving the planning efficiency of TAMP solvers for long-horizon manipulation tasks.

Although Learn2Decompose does not rely on predefined action abstractions for learning problem decomposition, we abstract actions to utilize TAMP solvers, which requires additional experts and efforts on the users. Another limitation arises from our use of the GNN-based scoring function. As noted by Silver et al. [9], this model struggles with open-domain tasks where the set of relevant objects is unknown. Moreover, while we can plan decomposed subproblems in parallel, the execution of these plans is sequential, due to the usage of only one robot arm, reducing the efficiency of real-world execution.

We aim to test our proposed methods in more scenarios, such as block stacking involving tool use for objects out of workspace, tasks that require contact-rich manipulation beyond pick-and-place operations, and tasks set in more realistic, human-centric environments. Regarding the limitations of our methods, future work could involve integrating LfD algorithms that can learn action abstraction from demonstrations like [43] to make our approach modeling-free, thus more user-friendly. Moreover, large/visual language models [44, 45, 46, 47] could potentially be used to infer the interesting object set, then improve the generalization ability of the GNN-based scoring function in handling open-domain tasks. We also want to integrate multi-robot path planning algorithms and task assignments methods to distribute the planned actions and motions to subsets of robots which can work simultaneously to improve the execution efficiency. Lastly, we aim to extend our methods to tackle long-horizon manipulation tasks in partially observable or dynamic environments where robust and fast replanning will be required to handle uncertainties and disturbances.

### **Acknowledgments**

This work was supported by the State Secretariat for Education, Research and Innovation in Switzerland for participation in the European Commissions Horizon Europe Program through the INTELLIMAN project (<https://intelliman-project.eu/>, HORIZON-CL4-Digital-Emerging Grant 101070136) and the SESTOSENSO project (<http://sestosenso.eu/>, HORIZON-CL4-Digital-Emerging Grant 101070310). We also acknowledge support from the SWITCH project (<https://switch-project.github.io/>), funded by the Swiss National Science Foundation.

## References

- [1] Z. Yang, C. Garrett, T. Lozano-Perez, L. Kaelbling, and D. Fox. Sequence-based plan feasibility prediction for efficient task and motion planning. In *Proc. Robotics: Science and Systems (RSS)*, 2023.
- [2] F. Suárez-Ruiz, X. Zhou, and Q.-C. Pham. Can robots assemble an ikea chair? *Science Robotics*, 3(17):eaat6385, 2018.
- [3] V. N. Hartmann, A. Orthey, D. Driess, O. S. Oguz, and M. Toussaint. Long-horizon multi-robot rearrangement planning for construction assembly. *IEEE Transactions on Robotics*, 39(1):239–252, 2022.
- [4] Y. Du, O. Watkins, Z. Wang, C. Colas, T. Darrell, P. Abbeel, A. Gupta, and J. Andreas. Guiding pretraining in reinforcement learning with large language models. In *Proc. Intl Conf. on Machine Learning (ICML)*, pages 8657–8677. PMLR, 2023.
- [5] N. Di Palo, A. Byravan, L. Hasenclever, M. Wulfmeier, N. Heess, and M. Riedmiller. Towards a unified agent with foundation models. In *Workshop on Reincarnating Reinforcement Learning at ICLR*, 2023.
- [6] C. R. Garrett, R. Chitnis, R. Holladay, B. Kim, T. Silver, L. P. Kaelbling, and T. Lozano-Pérez. Integrated task and motion planning. *Annual Review of Control, Robotics, and Autonomous Systems*, 4:265–293, 2021.
- [7] M. Toussaint. Logic-geometric programming: An optimization-based approach to combined task and motion planning. In *Intl Joint Conf. on Artificial Intelligence IJCAI*, pages 1930–1936, 2015.
- [8] C. R. Garrett, T. Lozano-Pérez, and L. P. Kaelbling. Pddlstream: Integrating symbolic planners and blackbox samplers via optimistic adaptive planning. In *Proc. of the Intl Conf. on Automated Planning and Scheduling*, volume 30, pages 440–448, 2020.
- [9] T. Silver, R. Chitnis, A. Curtis, J. B. Tenenbaum, T. Lozano-Pérez, and L. P. Kaelbling. Planning with learned object importance in large problem instances using graph neural networks. In *Proc. AAAI Conference on Artificial Intelligence*, volume 35, pages 11962–11971, 2021.
- [10] L. P. Kaelbling and T. Lozano-Perez. Hierarchical task and motion planning in the now. In *2011 IEEE International Conference on Robotics and Automation*, page 14701477, Shanghai, China, May 2011. IEEE. ISBN 978-1-61284-386-5.
- [11] A. Billard, S. Calinon, and R. Dillmann. Learning from humans. In B. Siciliano and O. Khatib, editors, *Handbook of Robotics*, chapter 74, pages 1995–2014. Springer, Secaucus, NJ, USA, 2016. 2nd Edition.
- [12] H. Friedrich, S. Munch, and R. Dillmann. Robot programming by demonstration (RPD): Supporting the induction by human interaction. 1996.
- [13] M. N. Nicolescu and M. J. Mataric. Natural methods for robot task learning: Instructive demonstrations, generalization and practice. In *Proc. of the Intl Joint Conf. on Autonomous Agents and Multiagent Systems*, pages 241–248, 2003.
- [14] A. Shah, P. Kamath, J. A. Shah, and S. Li. Bayesian inference of temporal task specifications from demonstrations. *Advances in Neural Information Processing Systems (NIPS)*, 31, 2018.
- [15] G. Chou, N. Ozay, and D. Berenson. Explaining multi-stage tasks by learning temporal logic formulas from suboptimal demonstrations. In *Proc. Robotics: Science and Systems (RSS)*, 2020.

- [16] B. Araki, J. Choi, L. Chin, X. Li, and D. Rus. Learning policies by learning rules. *IEEE Robotics and Automation Letters*, 7(2):12841291, Apr. 2022. ISSN 2377-3766, 2377-3774.
- [17] J. Yu, Y. Chai, Y. Wang, Y. Hu, and Q. Wu. CogTree: Cognition tree loss for unbiased scene graph generation. In *Proceedings of the Thirtieth International Joint Conference on Artificial Intelligence, IJCAI-21*, pages 1274–1280. International Joint Conferences on Artificial Intelligence Organization, 8 2021.
- [18] R. Li, S. Zhang, and X. He. Sgtr: End-to-end scene graph generation with transformer. In *proceedings of the IEEE/CVF conference on computer vision and pattern recognition*, pages 19486–19496, 2022.
- [19] Ö. Şimşek, A. P. Wolfe, and A. G. Barto. Identifying useful subgoals in reinforcement learning by local graph partitioning. In *Proc. Intl Conf. on Machine Learning (ICML)*, pages 816–823, 2005.
- [20] D. Tang, X. Li, J. Gao, C. Wang, L. Li, and T. Jebara. Subgoal discovery for hierarchical dialogue policy learning. In *Proc. of the Conf. on Empirical Methods in Natural Language Processing*, pages 2298–2309, 2018.
- [21] E. Chane-Sane, C. Schmid, and I. Laptev. Goal-conditioned reinforcement learning with imagined subgoals. In *Proc. Intl Conf. on Machine Learning (ICML)*, pages 1430–1440. PMLR, 2021.
- [22] T. Jurgenson, O. Avner, E. Groshev, and A. Tamar. Sub-goal trees a framework for goal-based reinforcement learning. In *Proc. Intl Conf. on Machine Learning (ICML)*, pages 5020–5030. PMLR, 2020.
- [23] M. Hong, M. Kang, and S. Oh. Diffused task-agnostic milestone planner. *Advances in Neural Information Processing Systems*, 36, 2024.
- [24] S. Levit, J. Ortiz-Haro, and M. Toussaint. Solving sequential manipulation puzzles by finding easier subproblems. In *Proc. IEEE Intl Conf. on Robotics and Automation (ICRA)*, May 2024.
- [25] M. J. McDonald and D. Hadfield-Menell. Guided imitation of task and motion planning. In *Conference on Robot Learning*, pages 630–640. PMLR, 2022.
- [26] M. Dalal, A. Mandlekar, C. R. Garrett, A. Handa, R. Salakhutdinov, and D. Fox. Imitating task and motion planning with visuomotor transformers. In *Conference on Robot Learning*, pages 2565–2593. PMLR, 2023.
- [27] B. Kim and L. Shimanuki. Learning value functions with relational state representations for guiding task-and-motion planning. In *Conf. on Robot Learning*, pages 955–968. PMLR, 2020.
- [28] D. Driess, O. Oguz, J.-S. Ha, and M. Toussaint. Deep visual heuristics: Learning feasibility of mixed-integer programs for manipulation planning. In *Proc. IEEE Intl Conf. on Robotics and Automation (ICRA)*, pages 9563–9569. IEEE, 2020.
- [29] S. Park, H. C. Kim, J. Baek, and J. Park. Scalable learned geometric feasibility for cooperative grasp and motion planning. *IEEE Robotics and Automation Letters*, 7(4):11545–11552, 2022.
- [30] M. Khodeir, B. Agro, and F. Shkurti. Learning to search in task and motion planning with streams. *IEEE Robotics and Automation Letters*, 8(4):19831990, Apr. 2023. ISSN 2377-3766, 2377-3774.
- [31] K. Leahy, A. Jones, and C.-I. Vasile. Fast decomposition of temporal logic specifications for heterogeneous teams. *IEEE Robotics and Automation Letters*, 7(2):2297–2304, 2022.

- [32] K. Elimelech, L. E. Kavraki, and M. Y. Vardi. Extracting generalizable skills from a single plan execution using abstraction-critical state detection. In *Proc. IEEE Intl Conf. on Robotics and Automation (ICRA)*, page 57725778, London, United Kingdom, May 2023. IEEE. ISBN 9798350323658.
- [33] K. Elimelech, Z. Kingston, W. Thomason, M. Y. Vardi, and L. E. Kavraki. Accelerating long-horizon planning with affordance-directed dynamic grounding of abstract strategies. In *IEEE International Conference on Robotics and Automation (ICRA)*, May 2024.
- [34] D. Driess, O. Oguz, and M. Toussaint. HLGP: hierarchical task and motion planning using logic-geometric programming. In *RSS Workshop on Robust Task and Motion Planning*, 2019.
- [35] R. Holladay, T. Lozano-Pérez, and A. Rodriguez. Robust planning for multi-stage forceful manipulation. *The International Journal of Robotics Research*, 43(3):330–353, 2024.
- [36] A. J. Ijspeert, J. Nakanishi, H. Hoffmann, P. Pastor, and S. Schaal. Dynamical movement primitives: learning attractor models for motor behaviors. *Neural computation*, 25(2):328–373, 2013.
- [37] M. Saveriano, F. J. Abu-Dakka, A. Kramberger, and L. Peternel. Dynamic movement primitives in robotics: A tutorial survey. *The International Journal of Robotics Research*, 42(13): 1133–1184, 2023.
- [38] S. Calinon. Programming industrial robots from few demonstrations. In *Human-Robot Collaboration: Unlocking the potential for industrial applications*, pages 9–37. Institution of Engineering and Technology (IET), 2023.
- [39] Y. Zhang, T. Xue, A. Razmjoo, and S. Calinon. Logic learning from demonstrations for multi-step manipulation tasks in dynamic environments. *IEEE Robotics and Automation Letters*, 9(8):7214–7221, 2024. doi:10.1109/LRA.2024.3418276.
- [40] P. Fournier-Viger, J. C.-W. Lin, R. U. Kiran, Y. S. Koh, and R. Thomas. A survey of sequential pattern mining. *Data Science and Pattern Recognition*, 1(1):54–77, 2017.
- [41] J. Pei, J. Han, B. Mortazavi-Asl, J. Wang, H. Pinto, Q. Chen, U. Dayal, and M.-C. Hsu. Mining sequential patterns by pattern-growth: The prefixspan approach. *IEEE Transactions on Knowledge and Data Engineering*, 16(11):1424–1440, 2004.
- [42] P. Fournier-Viger, J. C.-W. Lin, A. Gomariz, T. Gueniche, A. Soltani, Z. Deng, and H. T. Lam. The spmf open-source data mining library version 2. In *Machine Learning and Knowledge Discovery in Databases*, pages 36–40, Cham, 2016. Springer International Publishing. ISBN 978-3-319-46131-1.
- [43] S. Sharma, S. Tuli, and R. Paul. Unsupervised learning of neuro-symbolic rules for generalizable context-aware planning in object arrangement tasks. In *Proc. IEEE Intl Conf. on Robotics and Automation (ICRA)*, 2024.
- [44] R. Firoozi, J. Tucker, S. Tian, A. Majumdar, J. Sun, W. Liu, Y. Zhu, S. Song, A. Kapoor, K. Hausman, et al. Foundation models in robotics: Applications, challenges, and the future. *arXiv preprint arXiv:2312.07843*, 2023.
- [45] M. Ahn, A. Brohan, N. Brown, Y. Chebotar, O. Cortes, B. David, et al. Do as i can, not as i say: Grounding language in robotic affordances. *arXiv preprint arXiv:2204.01691*, 2022.
- [46] J. Xiang, T. Tao, Y. Gu, T. Shu, Z. Wang, Z. Yang, and Z. Hu. Language models meet world models: Embodied experiences enhance language models. *Advances in Neural Information Processing Systems*, 36, 2024.

- [47] D. Driess, F. Xia, M. S. M. Sajjadi, C. Lynch, A. Chowdhery, B. Ichter, et al. PaLM-e: An embodied multimodal language model. In *Proceedings of the 40th International Conference on Machine Learning*, volume 202 of *Proceedings of Machine Learning Research*, pages 8469–8488. PMLR, 2023.

## A Appendix

In this section, we provide supplementary details on details on PrefixSpan and the performance of GNN model, simulation and real-world experiments.

### A.1 Details on PrefixSpan

We employed PrefixSpan to extract subgoals that are defined by subgraph sets from demonstrations. Essentially, each subgraph was assigned as a unique integer variable. We then generated the sequential patterns of interest with the PrefixSpan implementation in [42] and set the *min\_support* to be 0.9 across all the experiments. The extracted sequential patterns, represented an integer variables, were subsequently mapped back to their corresponding subgraph sets and concatenated to form the subgoals.

Additionally, in processing the full graph representation of demonstrations, we ignored the geometrical states of each object and the static symbolic states, focusing primarily on the fluent predicates during the PrefixSpan deployment. This approach ensures that PrefixSpan concentrates on the dynamic symbolic states, avoiding unnecessary effort on static patterns within each sequence.

### A.2 Details on GNN-based Scoring Function.

We trained our GNN models with the implementation from [9]. We set the importance threshold  $\gamma = 0.8$  across all the experiments, identifying objects with importance scores over  $0.8$  as significant. The other hyperparameters for the GNN models were kept consistent with those specified in [9]. To ensure robust evaluation, we trained and tested the GNN models using different random seeds: seed 0 for collection demonstrations and seed 5 for generating the experimental results reported in Tables 1, 2, and 3.

	<b>Block4</b>	<b>Block6</b>	<b>Block8</b>	<b>Cook3</b>	<b>Cook4</b>	<b>Cook5</b>
<b>Time</b>	2.8	2.9	3.3	3.6	3.9	5.5
<b>Success</b>	100%	100%	99%	100%	100%	100%

Table 4: The planning accuracy and cost of the GNN model are evaluated in terms of average time cost (ms) and success rate for the tasks listed in Tables 1, 2 and 3.

In the table above, we report the average planning time and accuracy of the GNN models for each task listed in Tables 1, 2, and 3. Generally, the GNN models were capable of predicting the importance of objects in under six milliseconds. Besides, the GNN model accurately identified the important objects in all the experiments, with a single exception during one trial for the **Block8** task. We have included the planning time of this failure case in the result presented in Table 3.

### A.3 Simulation Experiments

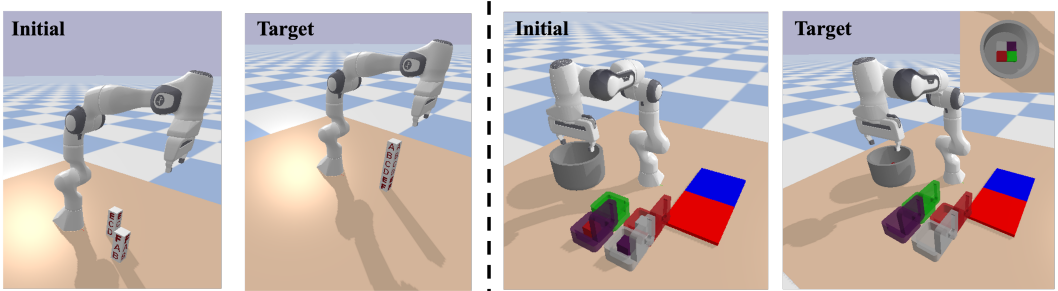


Figure 5: Illustrative experiment setups for the **Block6** (left) and **Cook4** (right) task. The initial states for both tasks are randomly sampled.

**Block-X Tasks.** To the left in Figure 5, the **Block6** task setup involves six blocks initially placed randomly on the table or stacked together, with the goal of stacking them in a specific order: *A on B on C on D on E on F*. The action set  $\mathcal{A}$  consists of *pick*, *place*, *unstack*, *stack*, each linked to a DMP model. These models are offline trained using a single motion-level demonstration to generalize the demonstrated trajectory for handling motion-level variants while concatenating plans for subproblems.

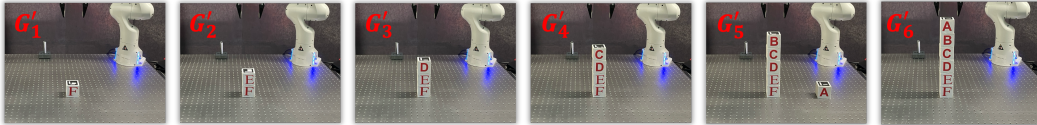
**Cook-X Tasks.** To the right in Figure 5, the **Cook4** task setup features four ingredients initially placed randomly in one of four ingredient boxes. The task goal is to prepare a meal with ingredients *green*, *purple*, *red*, and *pink*, cooked in sequential order. Random initial configuration may vary the status of boxes (*open* or *closed*), influencing the graspability of the ingredient inside. Each ingredient is also randomized with the status *washed* or *cut*. If an ingredient is not *washed* nor *cut*, then the robot arm needs to first *wash* it in the *sink* (blue large block) then *cut* it on the *cutting board* (red large block) before it can be *cooked* in the pot (grey cylinder). The action set  $\mathcal{A}$  includes *open*, *close*, *pick*, *wash*, *cut*, *cook*, and *cook-after*, with *cook-after* specifying sequential cooking order. *Open* and *close* adjust the status of ingredient boxes thus the graspability of ingredients inside. *Wash*, *cut*, and *cook* are simplified as a placing action in motion level. For instance, an ingredient is considered as *washed* or *cut*, if the robot arm *places* and *picks* it up from the cooker. We therefore used the trained DMPs in the **Block-X** tasks for *picking*, *washing*, *cutting*, and *cooking* in such tasks. To simplify, we assume that the box can open automatically, facilitating ingredient grasping. Please refer to the supplementary materials for illustrative videos of task accomplishment in both scenarios.

#### A.4 Real-world Experiments

We validated the effectiveness of our methods for **Block6** tasks under various initial states in real-world settings. All experiments were conducted using a 7-axis Franka robot arm, equipped with a RealSense D435 camera for object localization. The Learn2Decompose approach successfully decomposed the tasks into several subproblems and our parallelized hierarchical TAMP method concurrently found subplans for each subproblems, which were then concatenated to achieve the target tasks.

In the figures that follow, we illustrate the subgoals extracted from demonstrations, the defined subproblems, and the corresponding subplans for the random task showcased during the online phase in Figure 2. We also provided a detailed description of subgoals along with the initial and goal states of each subproblem. The symbols  $T$  and  $T'$  respectively represent the table and virtual table (a block where unimportant objects, represented with grey blocks in the following figures are virtually merged with the table), see supplementary material for additional demonstrations of these validation experiments.

Figure 6: Subgoals extracted from demonstrations of the **Block6** task



$G'_1$ : (*clear*,  $F$ ), (*ontable*,  $F$ ,  $T$ )

$G'_2$ : (*clear*,  $E$ ), (*onblock*,  $E$ ,  $F$ ), (*ontable*,  $F$ ,  $T$ )

$G'_3$ : (*clear*,  $D$ ), (*onblock*,  $D/E$ ,  $E/F$ ), (*ontable*,  $F$ ,  $T$ )

$G'_4$ : (*clear*,  $C$ ), (*onblock*,  $C/D/E$ ,  $D/E/F$ ), (*ontable*,  $F$ ,  $T$ )

$G'_5$ : (*clear*,  $B$ ), (*onblock*,  $B/C/D/E$ ,  $C/D/E/F$ ), (*ontable*,  $F$ ,  $T$ ), (*clear*,  $A$ ), (*ontable*,  $A$ ,  $T$ )

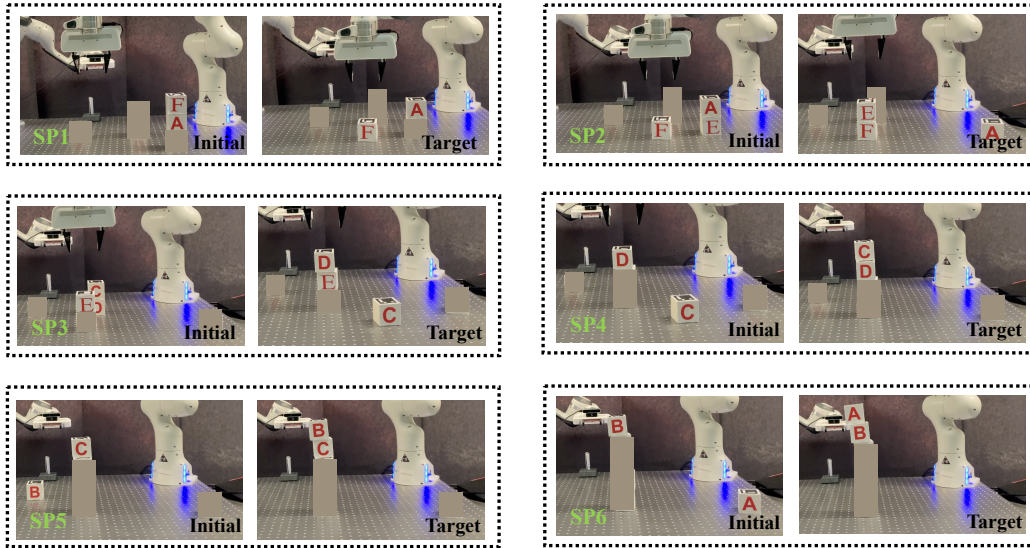
$G'_6$ : (*clear*,  $A$ ), (*onblock*,  $A/B/C/D/E$ ,  $B/C/D/E/F$ ), (*ontable*,  $F$ ,  $T$ )

SP<sub>1</sub>: Init: (*clear*,  $F$ ), (*onblock*,  $F$ ,  $A$ ), (*ontable*,  $A$ ,  $T'$ )

Goal: (*clear*,  $F$ ), (*ontable*,  $F$ ,  $T'$ ), (*ontable*,  $A$ ,  $T'$ )



Figure 7: Subproblems for reaching each subgoals of the **Block6** task



- SP<sub>2</sub>: Init: (*clear*, *A/F*), (*onblock*, *A, E*), (*ontable*, *E/F, T'*)  
 Goal: (*clear*, *A/E*), (*onblock*, *E, F*), (*ontable*, *A/F, T'*)
- SP<sub>3</sub>: Init: (*clear*, *C/E*), (*ontable*, *D/E, T'*), (*onblock*, *C, D*),  
 Goal: (*clear*, *C/D*), (*ontable*, *C/E, T'*), (*onblock*, *D, E*),
- SP<sub>4</sub>: Init: (*clear*, *C/D*), (*ontable*, *C/D, T'*)  
 Goal: (*clear*, *C*), (*ontable*, *D, T'*), (*onblock*, *C, D*)
- SP<sub>5</sub>: Init: (*clear*, *B/C*), (*ontable*, *B/C, T'*)  
 Goal: (*clear*, *B*), (*ontable*, *C, T'*), (*onblock*, *B, C*)
- SP<sub>6</sub>: Init: (*clear*, *A/B*), (*ontable*, *A/B, T'*)  
 Goal: (*clear*, *A*), (*ontable*, *B, T'*), (*onblock*, *A, B*)

Figure 8: Subplans generated concurrently with parallelized hierarchical TAMP for **Block6**.

